High electric permittivity of polymer-modified cement due to the capacitance of the interface between polymer and cement

Min Wang & D. D. L. Chung

Journal of Materials Science
Full Set - Includes `Journal of Materials Science Letters'

ISSN 0022-2461
Volume 53
Number 10

J Mater Sci (2018) 53:7199-7213
DOI 10.1007/s10853-018-2088-8

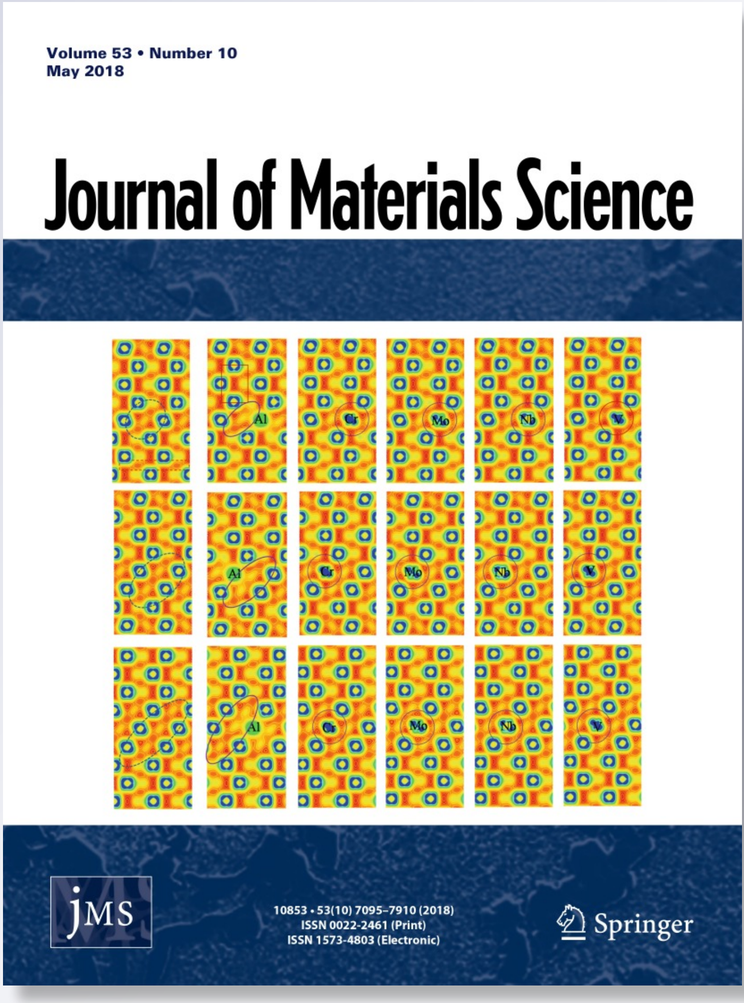

Springer

J Mater Sci (2018) 53:7199–7213

Ceramics

High electric permittivity of polymer-modified cement due to the capacitance of the interface between polymer and cement

Min Wang[1,2] and D. D. L. Chung[1,*]

[1] *Composite Materials Research Laboratory, Department of Mechanical and Aerospace Engineering, University at Buffalo, The State University of New York, Buffalo, NY 14260-4400, USA*

[2] *Present address: The Key Laboratory of Space Applied Physics and Chemistry, Ministry of Education and Shaanxi Key Laboratory of Macromolecular Science and Technology, School of Science, Northwestern Polytechnical University, Xi'an 710072, People's Republic of China*

Received: 18 November 2017
Accepted: 29 January 2018
Published online:
7 February 2018

ABSTRACT

The electric permittivity is a material property that relates to the dielectric and electromagnetic behaviors. This work reports the effect of polymer admixtures on the permittivity (2 kHz) of cement paste. The permittivity is increased significantly by the addition of either methylcellulose (dissolved) or latex (styrene–butadiene, not dissolved), due to the capacitance of the interface between polymer and cement. The permittivity is effectively modeled by a material-level equivalent circuit model that comprises cement, polymer and cement/polymer interface in parallel. The series model is not effective. For both methylcellulose and latex, the cement and cement/polymer interface dominate the contributions to the permittivity, while the polymer contributes little. The contributions of polymer and cement/polymer interface increase monotonically with increasing polymer/cement ratio, while the contribution of cement decreases monotonically. Methylcellulose at the highest proportion of 1.4% by mass of cement gives permittivity 52, whereas latex at the highest solid latex proportion of 14% by mass of cement gives permittivity 43. For the same polymer/cement ratio, the permittivity is much higher for methylcellulose than latex. The difference between methylcellulose and latex is due to the much greater contribution of the cement/polymer interface to the permittivity for methylcellulose than latex, as caused by the nanoscale morphology of the methylcellulose and the consequent large cement/polymer interface area. At the same polymer/cement ratio, the fractional contribution from the cement/polymer interface is greater for methylcellulose than latex, though those from the polymer and cement are greater for latex than methylcellulose.

Address correspondence to E-mail: ddlchung@buffalo.edu

https://doi.org/10.1007/s10853-018-2088-8

Springer

Introduction

The electric permittivity (the real part of the complex permittivity, also known as the dielectric constant) is a basic material property. It is a key to understanding the dielectric, ferroelectric, piezoelectric, pyroelectric, electric polarization and electromagnetic behaviors.

The piezoelectric behavior relates to the applications as strain/stress sensors (utilizing direct piezoelectric effect) and actuators (utilizing the converse piezoelectric effect) [1–4]. The pyroelectric behavior relates to the application as temperature and infrared sensors [5–7]. Due to the associated exchange interaction, ferroelectric behavior gives higher values of the permittivity than paraelectric behavior. A high value of the permittivity is attractive for providing high values of the piezoelectric coupling coefficient and pyroelectric coefficient. On the other hand, a low value of the permittivity is attractive for providing a high piezoelectric voltage coefficient.

The permittivity is also a key material property that governs the interaction of a material with electromagnetic radiation, such as radio wave. A high value of the permittivity is attractive for enhanced interaction with electromagnetic radiation, which is relevant to the use of electromagnetic radiation for nondestructive evaluation and object detection [8] and for electromagnetic interference (EMI) shielding [9–11].

The electric polarization behavior of a material affects the use of the electrical conductivity of the material, because the polarization causes a reverse electric field in the material [12, 13]. Furthermore, electric polarization is affected by stress, thus enabling polarization-based stress sensing [14]. The electrical conduction behavior relates to piezoresistivity-based strain/damage sensing [15–18], antistatic components [19], resistance-heating-based deicing [20, 21], electrical grounding and lightning protection. In addition, the conduction behavior relates to the cathodic protection of the steel embedded in concrete [22–25] and to the removal of ions (such as chloride ions) by electrochemical processes [25]. Although the electric permittivity is important for numerous functional properties, it has not been given adequate attention in the field of cement-based materials [6, 26–28]. The term "cement" refers to the hydrated cement throughout this paper, unless noted otherwise. Most prior work on the permittivity of cement-based materials concerns investigation of the process of hydration [29–32].

The relative permittivity of cement has been shown to be increased by latex addition [26, 33]. The addition to cement paste of latex (styrene–butadiene, 66% styrene, latex/cement mass ratio up to 0.30, where latex refers to the latex dispersion with 48 wt% latex solid) increases the relative permittivity at 2 kHz from 27 to 43. The increase occurs in spite of the low permittivity of latex solid compared to cement and is attributed to the interface between cement and latex solid [33]. The relative permittivity of silica fume cement has been shown to be increased from 21 to 54 at 10 kHz by the addition of short carbon fibers (0.5% by mass of cement, or 0.48 vol% of the cement paste) [26]. The relative permittivity of cement has been reported to be increased from 8 to 15 (1 kHz, 40 °C) by carbon nanofiber (1.2%) addition, such that the cement-based composite preparation unconventionally involves compaction of the cement mix [6].

Methylcellulose is a water-soluble polymeric admixture. The methylcellulose addition results in improved dispersion of the cement particles in the mix, in addition to a more uniform distribution of unhydrated cement particles in the matrix, such that there is no significant depletion near aggregate surfaces, thereby resulting in a reduction in the interfacial transition zone (ITZ) [34]. However, methylcellulose inhibits the hydration process of the cement clinker phases (such as C_3A) [35]. In particular, the addition of methylcellulose inhibits not only the formation of ettringite, but also the formation of monosulfate [36–38]. Methylcellulose addition causes the continued presence of gypsum after 24 h of hydration [36–38]. Moreover, the presence of methylcellulose results in a reduction in the reactivity of calcium sulfate dihydrate in the cement system [35]. In spite of an initial retardation of the hydration reactions, a higher degree of hydration is achieved with the presence of methylcellulose after 90 days of curing, due to the better dispersion of the cement particles in the water [39]. Methylcellulose (1% by mass of cement) addition results in a layered deposition of calcium hydroxide, arranged in stack without deformation, with polymer bridges between the layered calcium hydroxide crystals acting as a bonding agent between the layers, thereby improving the bonding and structure [36]. In addition, methylcellulose bridges between the layered crystals strengthen the microstructure [39]. Moreover, methylcellulose causes the formation of polymer films [37]. As a consequence, methylcellulose addition provides a more cohesive microstructure, with a reduced amount of microcracks [34, 39, 40]. Furthermore, the methylcellulose polymer network reduces the porosity in relation to both large and fine pores [41].

The solubility of methylcellulose in water provides a method of forming nanoscale methylcellulose, which can have various morphologies that include the fibrillar morphology [40, 42]. This solubility is in contrast to the insolubility of latex particles [33] and is attractive for facilitating its dispersion in cement. Due to the insolubility in water, latex particles tend to agglomerate around the hydrating C_3S grains and promote the formation of a composite microstructure [43]. The latex also tends to be adsorbed to the surfaces of cement particles, hydration crystals and other inorganic components [44–46], in addition to forming an interpenetrating network structure of latex and cement hydrate phases [47]. Furthermore, the latex retards the hydration in the early stage [48, 49]. The retardation is due to the sequestration of Ca^{2+} ions from the pore solution [50].

In the amount of 0.2–0.8% by mass of cement, methylcellulose addition increases the tensile strength, tensile ductility and compressive modulus, but decreases the tensile modulus, compressive strength and compressive ductility [51]. In addition, the addition of methylcellulose to cement paste containing silica fume enhances the viscous character of the resulting cured material, with the loss tangent increased by up to 50% and the storage modulus decreased by up to 14% [52]. Furthermore, the methylcellulose addition improves the bond strength between cement and stainless steel fiber [53], steel rebar [54] or carbon fiber [54] and enhances the dispersion of carbon fiber [55] and carbon nanofiber [56] in cement. Methylcellulose addition also decreases the thermal conductivity and increases the specific heat [57].

In spite of the above-mentioned prior work on the use of methylcellulose in cement-based materials, the effect of methylcellulose addition on the electric permittivity has not been previously reported. Due to the water-solubility of methylcellulose and the consequent polymer film formation [36, 39] and polymer network formation [41], the amount of interface between methylcellulose and cement is expected to be high (higher than that between latex and cement), thus leading to a high contribution of the interface to the electric permittivity.

Latex is much more commonly used in cement-based materials than methylcellulose. Latex-modified cement-based materials are attractive for their enhanced flexural strength [58–60], flexural toughness [60] and vibration damping ability [61], reduced void content [60] and improved adhesion and bonding properties [53, 62, 63]. However, the electrical behaviors of these materials have received little prior attention [60]. It has been reported that latex addition to cement increases both the electrical resistivity [60] and the electric permittivity [26]. The increase in resistivity is expected, since latex (a polymer) is an electrical insulator, while cement paste is conductive due to the ions present. However, the increase in electric permittivity is not expected, since the permittivity of latex (as typical for polymers) is lower than that of cement. It is reasonable to conjecture that polarization occurs at the interface between latex and cement, thereby causing the permittivity to be increased by the latex addition, as shown in our recent prior work [33].

The objectives of this work are (1) to investigate the effect of dissolved methylcellulose addition on the electric permittivity of cement, (2) to compare the effects of methylcellulose (dissolved, this work) and latex (not dissolved, prior work [33]), both as admixtures at various proportions, on the permittivity, (3) to understand the effects of methylcellulose and latex in terms of the contributions of cement, polymer and the interface between methylcellulose and cement on the permittivity, and (4) to provide a specimen-level equivalent circuit model to describe the electrical behavior of the polymer-modified cements.

Experimental methods

Materials

Portland cement (Type I, ASTM C150, unhydrated form) from Lafarge (Southfield, MI) is used. No aggregate is used. The water/cement mass ratio is fixed at 0.45, with the water including that in the latex dispersion in case that latex is used, and with the cement being that in the unhydrated form.

Methylcellulose (Dow Chemical, Midland, MI, Methocel A15-LV) is used in the amount ranging from 0.3 to 1.4% by mass of cement. A defoamer (Colloids, Inc., Marietta, GA, 1010) is used in the amount of 0.13 vol%, as in prior work [53–55, 57, 62], due to a small amount of bubbles generated by the addition of methylcellulose. Methylcellulose is first dissolved in water, and then, the defoamer is added and stirred by hand for 2 min.

The latex dispersion (#460NA, Dow Chemical, Midland, MI) has a styrene–butadiene copolymer with the polymer making up 48% of the dispersion mass and with the styrene and butadiene having a mass ratio of 66:34. An antifoaming agent (#2410, Dow Corning, Midland, MI) is used. The antifoam content is fixed at 0.5% by mass of latex dispersion. Firstly, the latex dispersion is mixed with the antifoam by hand for about 1 min. Secondly, the latex dispersion and water are mixed for 2 min.

The mix proportions for the case of latex are shown in Table 1. The mass ratio of the latex dispersion to cement ranges from 5.0 to 30.0%, whereas the mass ratio of the latex solid to cement ranges from 2.4 to 24.4%. As shown in Table 2, the mass ratio of methylcellulose to cement ranges from 0.3 to 1.4%. The volume fractions of the constituents (cement paste and polymer solid) are shown in Table 2 for both latex and methylcellulose.

The above-mentioned mixing is conducted using a rotary (Hobart) mixer with a flat beater. After the mixing, cement and water are added and further mixing is conducted for 5 min. Then, the mixture is poured into an oiled mold of dimensions 25 mm × 25 mm, immediately followed by covering the content of the mold with a wet towel in order to prevent loss of water. The specimens are demolded after 1 day and cured in air at room temperature (relative humidity = 100%) for the next 27 days.

Before capacitance measurement, the samples are burnished with water to ensure that the surfaces are smooth. No damage is caused by the burnishing. All three orthogonal dimensions are separately measured for each specimen after the burnishing.

Permittivity measurement and analysis method

Each specimen tested is a square of dimensions 25 mm × 25 mm, with thickness ranging from about 2 mm to about 4 mm. The aspect ratio is large enough for the fringing field to be small enough, so that the permittivity determination is reliable, as shown in the prior work of this research group [27].

The permittivity is measured using the parallel-plate capacitor geometry, with two electrical contacts sandwiching the specimen symmetrically. An electrical contact (copper foil of thickness 0.15 mm) covers the entire area of each of the two square surfaces of the specimen. Between each of the two copper foils and the specimen is positioned an electrically insulating Teflon-coated glass fiber composite film (thickness 58 μm, relative permittivity 1.5 at 2 kHz). The configuration is illustrated in Fig. 1. The importance of using an insulating film has been noted previously [64]. Instead of using an insulating film, an air gap of 0.25 mm has also been used in prior work [65]. However, an air gap is associated with a very large resistance, so that the electric field experienced by the cement specimen would become too small for adequate capacitance measurement. In fact, it is important for the insulating film to be thin enough, so that the resistance is not too high. A pressure of 9.93 kPa is applied in the direction perpendicular to the plane of the sandwich.

The capacitance is measured using a precision RLC meter (Instek LCR-816 High Precision LCR Meter, 100 Hz-2 kHz), with the electric field across the thickness of the specimen fixed at 0.10 V/mm. The voltage is increased with the specimen thicknesses; for example, for a specimen thickness of 3.90 mm, the

Table 1 Mix proportions for the latex-modified cement-based materials studied

Latex dispersion/cement mass ratio	Latex solid/cement mass ratio	Cement (g)	Latex dispersion (g)	Water (g)	Antifoam (g)
0	0	100.0 ± 0.5	0	45.0 ± 0.05	0
0.05	0.024	100.0 ± 0.5	5.0 ± 0.5	42.4 ± 0.05	0.025
0.10	0.048	100.0 ± 0.5	10.0 ± 0.5	39.8 ± 0.05	0.050
0.15	0.072	100.0 ± 0.5	15.0 ± 0.5	37.2 ± 0.05	0.075
0.20	0.096	100.0 ± 0.5	20.0 ± 0.5	34.6 ± 0.05	0.100
0.25	0.120	100.0 ± 0.5	25.0 ± 0.5	32.0 ± 0.05	0.125
0.30	0.144	100.0 ± 0.5	30.0 ± 0.5	29.4 ± 0.05	0.150

Table 2 Volume fraction of cement paste and the volume fraction of polymer solid in the cured cement paste for latex and that with methylcellulose

Polymer/cement mass ratio		Volume fraction of cement paste		Volume fraction of polymer solid	
Latex dispersion/cement mass ratio	Methylcellulose/cement mass ratio	Latex	Methylcellulose	Latex	Methylcellulose
0	0	1	1	0	0
0.050	0.003	0.962 ± 0.005	0.996 ± 0.005	0.0376 ± 0.0005	0.0035 ± 0.0005
0.100	0.004	0.927 ± 0.005	0.995 ± 0.005	0.0726 ± 0.0005	0.0046 ± 0.0005
0.150	0.005	0.895 ± 0.005	0.994 ± 0.005	0.1050 ± 0.0005	0.0058 ± 0.0005
0.200	0.006	0.865 ± 0.005	0.993 ± 0.005	0.1353 ± 0.0005	0.0069 ± 0.0005
0.250	0.007	0.836 ± 0.005	0.992 ± 0.005	0.1636 ± 0.0005	0.0081 ± 0.0005
0.300	0.008	0.810 ± 0.005	0.991 ± 0.005	0.1900 ± 0.0005	0.0092 ± 0.0005
/	0.009	/	0.990 ± 0.005	/	0.0103 ± 0.0005
/	0.010	/	0.988 ± 0.005	/	0.0115 ± 0.0005
/	0.011	/	0.987 ± 0.005	/	0.0126 ± 0.0005
/	0.012	/	0.986 ± 0.005	/	0.0138 ± 0.0005
/	0.013	/	0.985 ± 0.005	/	0.0149 ± 0.0005
/	0.014	/	0.984 ± 0.005	/	0.0160 ± 0.0005

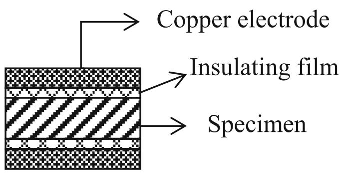

Figure 1 Configuration for measuring the relative permittivity of a cement-based specimen. An electrically insulating film is positioned between the specimen and each of the two sandwiching copper electrodes. The drawing is not too scale, as the specimen dimension is much smaller in the vertical direction than the horizontal direction.

voltage is 0.39 V. The frequency used is 2 kHz, because it is the highest frequency provided by the LCR meter used. Lower frequencies give consistent results, though the results are clearest at the highest frequency. The capacitance reported here is for the equivalent electrical circuit of a capacitance and a resistance in parallel.

The methodology for measuring the capacitance involves firstly the separation of the interfacial capacitance (interface between the specimen and an electrical contact) from the volumetric capacitance (the volume of the specimen). This decoupling is enabled by the testing of three different thicknesses of the sandwiched specimen and plotting the inverse of the measured capacitance C_m versus thickness l. The slope of the straight-line plot is equal to $1/(\kappa\varepsilon_o A)$, where κ is the relative permittivity of the specimen, ε_o is the permittivity of free space, and A is the area of the sandwiched dielectric material. Hence, κ is obtained from the reciprocal of the slope. The intercept of the straight with the vertical axis at zero thickness equals $2/C_i$, where C_i is the capacitance of one interface. In other words,

$$1/C_m = 1/C_v + 2/C_i, \tag{1}$$

where C_v is the volumetric capacitance. Using Eq. (1), which is based on capacitors in series, $1/C_v$ is obtained for a given value of l. The C_v is given by

$$C_v = \varepsilon_o \kappa A/l, \tag{2}$$

where ε_o is the permittivity of free space (8.85×10^{-12} F/m), A is the area of the sandwich (i.e., the area of the electrical contact), and l is the thickness of the specimen sandwiched by the electrical contacts.

The cement, polymer (methylcellulose or latex) solid and the interface between these components are modeled electrically as continuous dielectric components that are either in parallel or in series, with capacitances C_C, C_P and C_I, respectively. This dielectric continuity assumption is consistent with the results of prior work on the film and network structure of cement containing methylcellulose [54, 58] and is supported by the previously reported nanoscale fibrillar morphology of the methylcellulose

[36, 38]. With the cement and polymer solid components alternating in their positions (Fig. 2), let N be the number of cement layers. Then, the number of polymer solid layers is $N-1$ and the number of cement/polymer interfaces is $2N-2$.

In the specimen-level parallel model (Fig. 2a), according to the rule of mixtures [66],

$$C_v = NC_C + (N-1)C_P + (2N-2)C_I. \quad (3)$$

Rearrangement of Eq. (3) and the use of Eq. (2) give the contribution κ_I of the interfaces to the relative permittivity of the cement-based material as

$$\kappa_I = (2N-2)\frac{C_I l}{A\varepsilon_0} = \kappa - V_C\kappa_C - V_P\kappa_P, \quad (4)$$

where V_C and κ_C are the volume fraction and relative permittivity of cement, respectively, and V_P and κ_P are the volume fraction and relative permittivity of the polymer solid, respectively. The terms $V_C\kappa_C$and$V_P\kappa_P$ are the contributions of the cement and polymer solid to the relative permittivity of the cement-based material, respectively. The volume fractions are obtained from the mass fractions and the densities.

The density of cement is taken as 1.62 g/cm^3, which is the density of the cement-based material without polymer addition, as measured in this work.

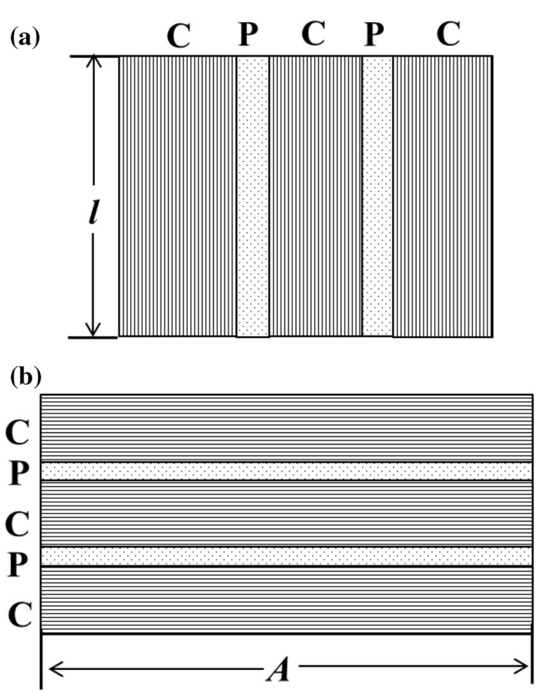

Figure 2 Material-level equivalent electric circuit models for the cement-based materials of this work. C = cement; P = polymer solid. **a** Parallel model. **b** Series model.

For the methylcellulose solid, the density is 1.39 g/cm^3 [67] and the relative permittivity is 3.0 [68]. The density of latex solid (with 66% styrene) is taken as 0.994 g/cm^3, which is obtained by extrapolating the known densities of styrene–butadiene of 0.965 g/cm^3 at 45% styrene and 0.910 g/cm^3 for 5% styrene [69]. The relative permittivity of styrene–butadiene solid is 2.8 [70].

In the specimen-level series model (Fig. 2b), according to the rule of mixtures [66],

$$1/C_v = N/C_C + (N-1)/C_P + (2N-2)/C_I. \quad (5)$$

Rearrangement of Eq. (5) and the use of Eq. (2) give the contribution $1/\kappa_I$ of the interfaces to the reciprocal of the relative permittivity of the cement-based material as

$$1/\kappa_I = (2N-2)\frac{A\varepsilon_0}{C_I l} = 1/\kappa - V_C/\kappa_C - V_L/\kappa_P. \quad (6)$$

The terms V_C/κ_C and V_P/κ_P are the contributions of the cement and polymer solid to the reciprocal of the relative permittivity of the cement-based material, respectively.

This work uses a technique which differs greatly from the widely used technique of impedance spectroscopy, which measures the impedance as a function of frequency and uses the frequency dependence to obtain information. Firstly, the technique of this work does not measure the impedance, but measures the relative permittivity (the real part of the permittivity). In connection with permittivity measurement, this work measures the capacitance with a test configuration in which an insulating film is positioned between the specimen and each of the two electrodes. The presence of this film ensures that the resistance of the system is high enough for the measured capacitance given by the LCR is correct. However, the presence of this film would cause the specimen resistance to be not effectively measured. Resistance measurement is not a part of this study. An insulating film is not usually used in impedance spectroscopy, thus causing the capacitance measurement in the impedance spectroscopy to be questionable. Secondly, the technique of this work decouples the contribution of the specimen–contact interface from the contribution of the volume of the specimen, as achieved by testing specimens of the same type at three different thicknesses and plotting the reciprocal of the measured capacitance versus the thickness (Fig. 3). The slope of this plot relates to the

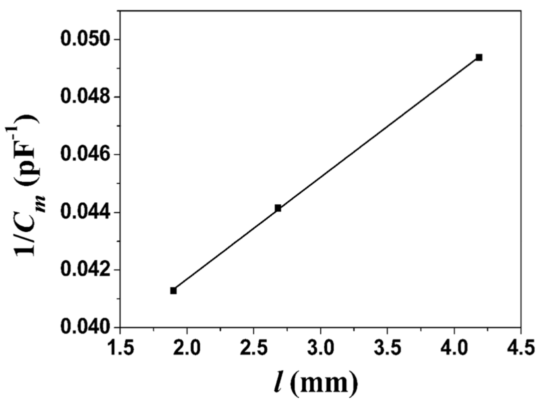

Figure 3 Plot of $1/C_m$ versus thickness l for the specimen with methylcellulose/cement ratio 0.012, where C_m is the measured capacitance.

permittivity of the specimen, with the specimen–contact interface contribution to the measured capacitance removed. This decoupling is not adequately performed in impedance spectroscopy, as explained below. Thirdly, the technique of this work uses a system-level equivalent circuit model (Fig. 4, which is drawn for the case of the specimen-level parallel model shown in Fig. 2a) that includes the specimen and the two electrical contacts and reflects the testing configuration, in which the specimen is in series with two electrical contacts on its two sides, such that each of the specimen and electrical contacts consists of a resistance and a capacitance in parallel. This system-level circuit model is intended to explain the method of testing rather than the method of

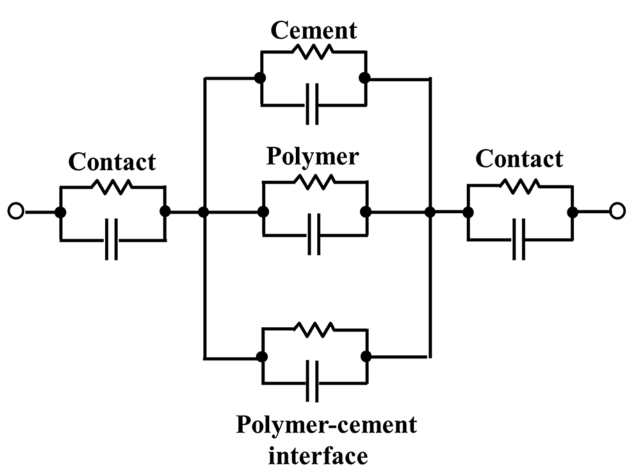

Figure 4 System-level equivalent circuit model with the specimen consisting of cement, polymer solid and polymer/cement interface in series with two electrical contacts on the two sides of the specimen. This model is drawn for the material-level parallel model (Fig. 2a) for the specimen.

analysis. The testing includes the decoupling of the specimen contribution and the contact contribution and also includes having the LCR meter set for resistance and capacitance in parallel. In this work, only the volumetric and contact capacitances in the system-level model are measured; the volumetric and contact resistances are not measured. None of the values of the circuit elements is obtained by calculation, but the values are obtained by direct measurement. Fourthly, the technique of this work does not need to address the frequency dependence in order to obtain meaningful information. In contrast, impedance spectroscopy is focused on the frequency dependence of the impedance, as conventionally described in terms of the Nyquist plot, for the purpose of deriving by mathematical fitting of the plot an equivalent electrical circuit that is intended to describe the electrical/dielectric behavior of the material. The system-level circuit model obtained by the curve fitting [71] tends to be not unique, so the determined values of the circuit elements (including the interfacial and volumetric elements) in the model are not very meaningful [72, 73].

Results and discussion

Effect of methylcellulose on the permittivity

Figure 3 shows that the experimental plot of $1/C_m$ versus l is indeed linear, as observed for all of the cement-based materials studied. Table 3 shows that the relative permittivity κ of the cement-based material increases monotonically with increasing methylcellulose/cement ratio. The value is increased from 27 (for the absence of methylcellulose) to 52 (for the highest methylcellulose/cement ratio of 0.012). The value of 27 for the absence of methylcellulose is in agreement with prior work [26, 33]. Linearity is obtained for all the polymer-modified cement-based materials of this work, whether the polymer is methylcellulose or latex.

Comparison of the effects of methylcellulose and latex on the permittivity

Latex is a commonly used polymeric admixture that is not soluble in water. The effect of latex (styrene–butadiene copolymer) addition on the permittivity

Table 3 Effect of the methylcellulose/cement ratio on the relative permittivity κ of the cement-based material

Ratio[a]	0	0.003	0.004	0.005	0.006	0.007	0.008	0.009	0.010	0.011	0.012	0.013	0.014
κ	26.98 ± 0.90	30.13 ± 0.78	31.86 ± 0.49	33.49 ± 0.53	36.16 ± 1.16	37.66 ± 0.08	39.27 ± 0.28	42.03 ± 0.74	43.76 ± 0.49	46.36 ± 0.78	48.86 ± 1.26	50.22 ± 0.31	51.65 ± 1.34

[a] Methylcellulose/cement ratio

has been addressed in our prior work [33]. This section compares the effects of dissolved methylcellulose (this work) and undissolved latex (prior work) on the permittivity. For both methylcellulose and latex, the polymer in the polymer/cement mass ratio refers to the polymer solid. This is in contrast to our prior work on latex [33], which uses the mass of the latex particle water-based dispersion in the latex/cement ratio. The highest polymer/cement ratio used in the study is much higher for latex than methylcellulose, in accordance with the common ranges of this ratio used in prior work for these two polymeric admixtures [36, 41, 55].

As shown in Fig. 5, for both methylcellulose and latex, the relative permittivity increases monotonically with increasing polymer/cement ratio. At the same polymer/cement ratio, the relative permittivity is much higher for methylcellulose than latex. Even at the highest latex/cement ratio of 0.14, the relative permittivity (43) is lower than the value (52) for the highest methylcellulose/cement ratio of 0.012. The high values of the relative permittivity for methylcellulose can be understood through material-level modeling of the permittivity using the parallel model of the rule of mixtures, as described below in terms of both the parallel model and the series model.

As shown in Fig. 6a, the contribution of the cement matrix to the measured relative permittivity, according to the material-level parallel model, decreases with increasing polymer/cement ratio for both methylcellulose and latex, as expected. The data for the two polymers lie essentially on the same

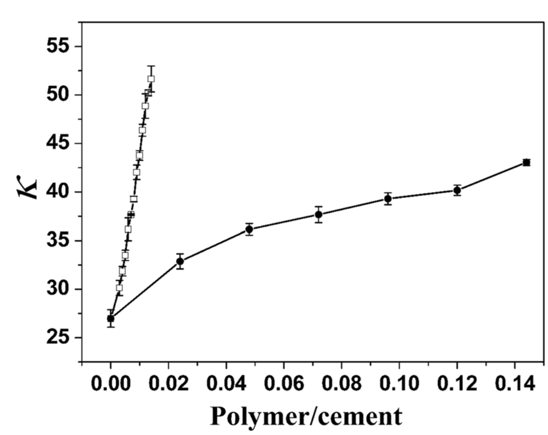

Figure 5 Effect of the polymer/cement mass ratio on the measured relative permittivity κ. Open square: methylcellulose. Filled circle: latex.

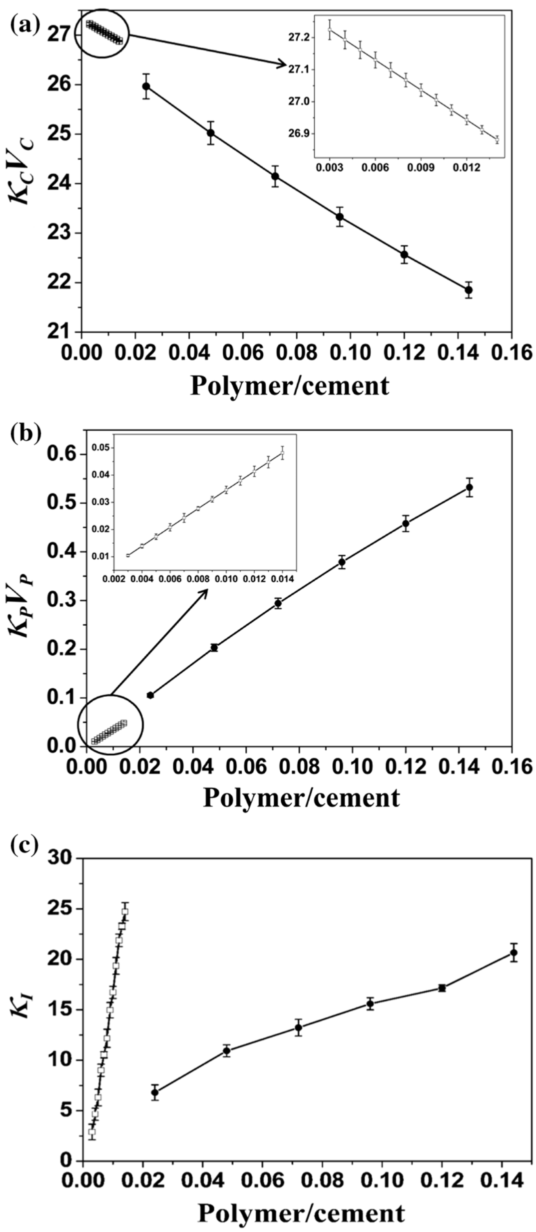

Figure 6 Effect of the polymer/cement mass ratio on the contributions to the measured relative permittivity κ, according to the material-level parallel model (Fig. 2a). **a** The contribution $\kappa_C V_C$ of the cement. **b** The contribution $\kappa_P V_P$ of the polymer. **c** The contribution $\kappa_I = (2N-2)\frac{C_I l}{A\varepsilon_0}$ of the interface between cement and polymer. Open square: methylcellulose. Filled circle: latex.

curve, supporting the effectiveness of the material-level parallel model. Due to the low values of the methylcellulose/cement ratio compared to the latex/cement ratio, the contribution of the cement matrix is higher for methylcellulose than latex.

As shown in Fig. 6b, the contribution of the polymer to the measured relative permittivity, according to the material-level parallel model, increases with increasing polymer/cement ratio for both methylcellulose and latex, as expected. The data for the two polymers lie essentially on the same curve, supporting the effectiveness of the material-level parallel model. Due to the low values of the methylcellulose/cement ratio compared to the latex/cement ratio, the contribution of the polymer is lower for methylcellulose than latex.

As shown in Fig. 6c, the contribution of the cement/polymer interface to the measured relative permittivity, according to the material-level parallel model, increases with increasing polymer/cement ratio for both methylcellulose and latex, as expected. The data for the two polymers lie on the different curves, with the slope of the curve for methylcellulose being higher than that for the curve for latex. Furthermore, the highest value for methylcellulose is above that for latex, in spite of the low methylcellulose content. These results mean that methylcellulose is more effective than latex for providing cement/polymer interface that enhances the permittivity of the cement-based material. In other words, even at a lower value of the polymer/cement ratio, methylcellulose provides comparable or greater interface-induced permittivity than latex. This is attributed to the nanostructure of the methylcellulose and the consequent large area of the cement/polymer interface per unit volume.

The fractional contributions of the cement, polymer and cement/polymer interface to the permittivity are shown in Fig. 7. Figure 7a shows that the fractional contribution of the cement is comparable for methylcellulose and cement. The highest value for methylcellulose is higher than that of latex. These occur though the polymer/cement ratio is much lower (i.e., the cement/polymer ratio is much higher) for methylcellulose than latex. Extrapolation of the curve for latex to lower values of the polymer/cement ratio suggests that, at the same polymer/cement ratio, the fractional contribution of the cement is greater for latex than methylcellulose. This means that the cement is a less efficient contributor in the presence of methylcellulose than in the presence of latex. This difference between methylcellulose and latex is probably due to the nanostructure of methylcellulose and the consequent reduced degree

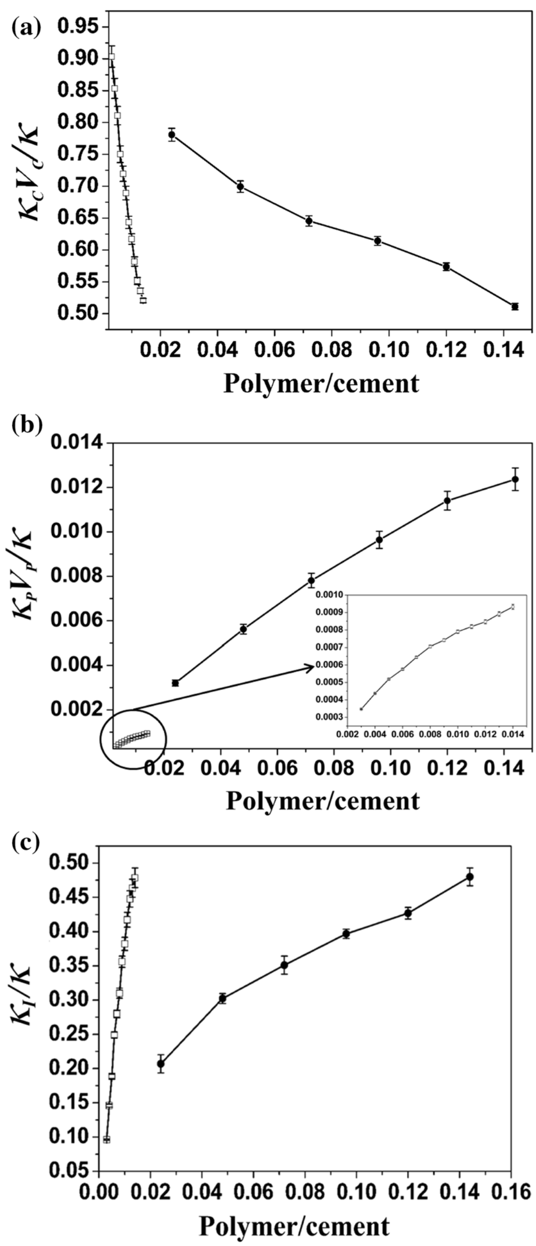

Figure 7 Effect of the polymer/cement mass ratio on the fractional contributions to the measured relative permittivity κ, according to the material-level parallel model (Fig. 2a). **a** The fractional contribution of the cement. **b** The fractional contribution of the polymer. **c** The fractional contribution $\kappa_I/\kappa = (2N - 2)\frac{C_I l}{\kappa A \varepsilon_0}$ of the interface between cement and polymer. Open square: methylcellulose. Filled circle: latex.

of dielectric continuity of the cement caused by the distributed nanoscale methylcellulose.

Figure 7b shows that the fractional contribution from the polymer is much lower for methylcellulose than latex. Extrapolation of the curve for latex to lower values of the polymer/cement ratio suggests that, for the same polymer/cement ratio, the fractional contribution from the polymer is greater for latex than methylcellulose.

Figure 7c shows that the fractional contribution from the cement/polymer interface is comparable for methylcellulose and latex, in spite of the much smaller polymer/cement ratio for methylcellulose than latex. Extrapolation of the curve for latex to lower values of the polymer/cement ratio suggests that, for the same polymer/cement ratio, the fractional contribution from the interface is greater for methylcellulose than latex. This difference between methylcellulose and latex is probably due to the nanostructure of the methylcellulose and the consequence large area of the cement/polymer interface for methylcellulose. Hence, the superior effectiveness of methylcellulose compared to latex for increasing the permittivity (Fig. 5) is due to the cement/polymer interface.

Figure 8 shows the effect of the polymer/cement mass ratio on the contributions of the cement, polymer and cement/polymer interface to the reciprocal $1/\kappa$ of the measured relative permittivity, according to the material-level series model. The contribution $1/\kappa_I = (2N - 2)\frac{\varepsilon_0 A}{C_I l}$ of the cement/polymer interface, as shown in Fig. 8c, is negative. The negative value is not reasonable, indicating the seriously inadequate effectiveness of the material-level series model. Nevertheless, the contribution of the cement decreases with increasing polymer/cement ratio, and the contribution of the polymer increases with increasing polymer/cement ratio, as in Fig. 7, which is obtained by using the material-level parallel model. The inadequate effectiveness of the material-level series model may stem from the fact that the permittivity is measured along the thickness (shortest dimension) of the specimen and the greater chance for the polymer films to be tortuously dielectrically continuous along this short dimension than along the long dimension perpendicular to the thickness direction, even if the polymer films are randomly oriented. In other words, the chance of attaining a tortuously dielectrically continuous path is higher when the distance over which dielectric continuity is required is shorter.

The parallel and series material-level models are the two most basic material-level models for calculating the relative permittivity of a composite material. Both material-level models have been

Figure 8 Effect of the polymer/cement mass ratio on the contributions to the reciprocal $1/\kappa$ of the measured relative permittivity, according to the material-level series model (Fig. 2b). **a** The contribution V_C/κ_C of the cement. **b** The contribution V_P/κ_P of the polymer. **c** The contribution $1/\kappa_I = (2N-2)\frac{\varepsilon_0 A}{C_I l}$ of the interface between cement and polymer. Open square: methylcellulose. Filled circle: latex.

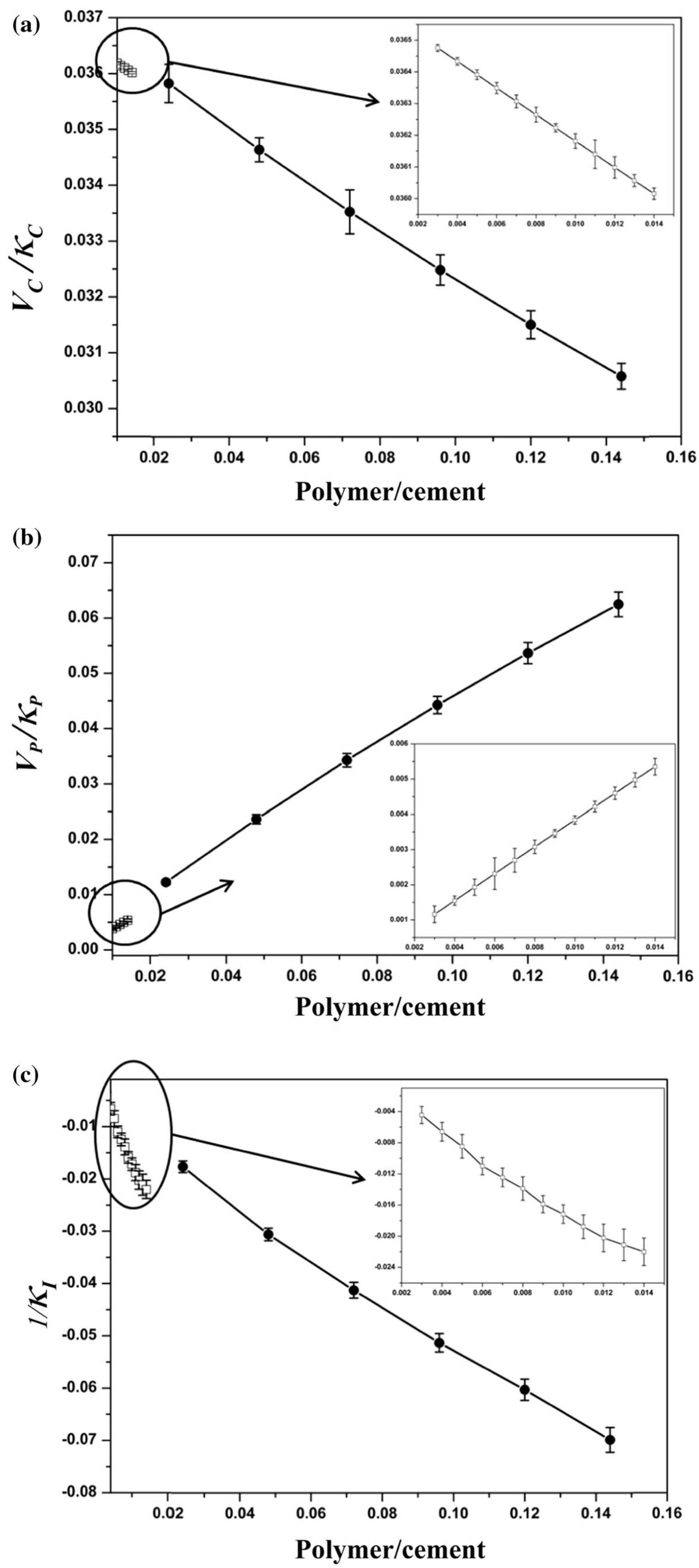

investigated in this work, but the material-level parallel model is found to give more meaningful results than the material-level series model. Both material-level models assume dielectric continuity of the constituents, i.e., cement, polymer and the cement/polymer interface. A degree of dielectric continuity of the polymer is supported by the previously reported polymer film formation in a cement-based material [54]. More accurately, the calculated value of the permittivity should be taken as being bound by the calculated value based on the material-level parallel model and that based on the material-level series model [74]. However, the former value alone is used in this work, due to the seriously inadequate effectiveness of the material-level series model and the above-mentioned higher chance of attaining a tortuously dielectrically continuous path in the measurement direction of shorter distance than the transverse direction of much longer distance.

The superior effectiveness of methylcellulose compared to latex for increasing the permittivity of cement is consistent with the superior effectiveness of methylcellulose compared to latex for increasing the vibration damping ability [56], bond strength of cement with steel [36] and degree of carbon fiber dispersion [39], and for decreasing the thermal conductivity [41]. Methylcellulose in the amount of 0.4% by mass of cement is comparable to latex in the amount of 20% by mass of cement in the effectiveness for enhancing the vibration damping ability of cement [56]. Methylcellulose in the amount of 0.8% by mass of cement is comparable to latex in the amount of 25% by mass of cement in the effectiveness for decreasing the thermal conductivity of cement [41]. Methylcellulose in the amount of 0.4% by mass of cement is better than latex in the amount of 20% by mass of cement in the effectiveness for enhancing the degree of carbon fiber dispersion in cement [39]. In addition, methylcellulose in the amount of 0.4% by mass of cement is comparable to latex in the amount of 20% by mass of cement in the effectiveness for enhancing the bond strength of cement to steel fiber [36].

Conclusion

This work provides the effect of polymer admixtures on the electric permittivity (2 kHz) of cement paste. The measurement involves measuring the capacitance of specimens of three thicknesses for each composition, so that the contributions of the specimen and the interface between the specimen and each electrical contact are decoupled. For every composition, the curve of $1/C$ (where C is the measured capacitance) versus thickness is linear.

The permittivity is increased significantly by the addition of either methylcellulose (dissolved) or latex (styrene–butadiene, not dissolved) to cement paste, due to the capacitance of the interface between polymer and cement. The permittivity is effectively modeled in the material level by an equivalent circuit model that comprises cement, polymer and cement/polymer interface in parallel. The material-level series model is not effective. For both methylcellulose and latex, cement and the cement/polymer interface dominate the contributions to the permittivity, while the polymer contributes much less. The contribution of polymer to the permittivity and that of the cement/polymer interface increase monotonically with increasing polymer/cement ratio, while the contribution of cement decreases monotonically.

For the same polymer/cement ratio, the permittivity is much higher for methylcellulose than latex. Methylcellulose at the highest proportion of 1.4% by mass of cement gives permittivity 52, whereas latex at the highest solid latex proportion of 14.4% by mass of cement gives permittivity 43.

The difference between methylcellulose and latex in their effects to the permittivity is due to the much greater contribution of the cement/polymer interface to the permittivity for methylcellulose than latex, as caused by the nanoscale morphology of the methylcellulose and the consequent large cement/polymer interface area. At the same polymer/cement ratio, the fractional contribution from the cement/polymer interface is greater for methylcellulose than latex, though the fractional contribution from the polymer is greater for latex than methylcellulose, and the fractional contribution of the cement is greater for latex than methylcellulose.

The superior effectiveness of methylcellulose compared to latex for increasing the permittivity of cement is consistent with the superior effectiveness of methylcellulose compared to latex for increasing the vibration damping ability [56], bond strength of cement with steel [36] and degree of carbon fiber dispersion [39], and for decreasing the thermal conductivity [41].

Compliance with ethical standards

Conflict of interest The authors declare that they have no conflict of interest.

References

[1] Ramam K, Chandramouli K (2012) Piezoelectric cement composite for structural health monitoring. Adv Cem Res 24:165–171

[2] Shen B, Yang X, Li Z (2006) A cement-based piezoelectric sensor for civil engineering structure. Mater Struct (Dordrecht, Netherlands) 39:37–42

[3] Lam KH, Chan HLW (2005) Piezoelectric cement-based 1-3 composites. Appl Phys A 81:1451–1454

[4] Zhang D, Li Z, Wu K (2002) 2-2 Piezoelectric cement matrix composite: part II. Actuator effect. Cem Concr Res 32:825–830

[5] Wen S, Chung DDL (2003) Pyroelectric behavior of cement-based materials. Cem Concr Res 33(10):1675–1679

[6] Batra AK, Bhattacharjee S, Chilvery AK, Aggarwal MD, Edwards ME, Bhalla A (2011) Simulation of energy harvesting from roads via pyroelectricity. J Photonics Energy 1:014001

[7] Bhat KN, Batra AK, Bhattacharjee S, Taylor RW (2010) Effect of volcanic-ash on the pyroelectric and dielectric properties of Portland cement. Proc SPIE 7780(Detectors and Imaging Devices):77800L/1–77800L/7

[8] Van Den Bril K, Gregoire C, Swennen R, Lambot S (2007) Ground-penetrating radar as a tool to detect rock heterogeneities (channels, cemented layers and fractures) in the Luxembourg Sandstone Formation (Grand-Duchy of Luxembourg). Sedimentology 54:949–967

[9] Muthusamy S, Chung DDL (2010) Carbon fiber cement-based materials for electromagnetic interference shielding. ACI Mater J 107:602–610

[10] Cao J, Chung DDL (2004) Use of fly ash as an admixture for electromagnetic interference shielding. Cem Concr Res 34:1889–1892

[11] Wen S, Chung DDL (2004) Electromagnetic interference shielding reaching 70 dB in steel fiber cement. Cem Concr Res 34:329–332

[12] Cao J, Chung DDL (2004) Electric polarization and depolarization in cement-based materials, studied by apparent electrical resistance measurement. Cem Concr Res 34:481–485

[13] Wen S, Chung DDL (2001) Electric polarization in carbon fiber reinforced cement. Cem Concr Res 31:141–147

[14] Wen S, Chung DDL (2001) Effect of stress on the electric polarization in cement. Cem Concr Res 31:291–295

[15] Wen S, Chung DDL (2007) Piezoresistivity-based strain sensing in carbon fiber reinforced cement. ACI Mater J 104:171–179

[16] Zhu S, Chung DDL (2007) Theory of piezoresistivity for strain sensing in carbon fiber reinforced cement under flexure. J Mater Sci 42:6222–6233. https://doi.org/10.1007/s10853-006-1131-3

[17] Wen S, Chung DDL (2003) A comparative study of steel- and carbon-fiber cement as piezoresistive strain sensors. Adv Cem Res 15:119–128

[18] Chung DDL (2002) Piezoresistive cement-based materials for strain sensing. J Intell Mater Syst Struct 13:599–609

[19] Shalaby A, Ward A, Refaee A, Abd-El-Messieh S, Abd-El-Nour K, El-Nashar D, Zayed H (2013) Compressive strength and electrical properties of cement paste utilizing waste polyethylene terephthalate bottles. J Appl Sci Res 9:4160–4173

[20] Chang C, Ho M, Song G, Mo Y, Li H (2009) A feasibility study of self-heating concrete utilizing carbon nanofiber heating elements. Smart Mater Struct 18:127001/1–127001/5

[21] Wang S, Wen S, Chung DDL (2004) Resistance heating using electrically conductive cements. Adv Cem Res 16:161–166

[22] Hou J, Chung DDL (1997) Cathodic protection of steel reinforced concrete facilitated by using carbon fiber reinforced mortar or concrete. Cem Concr Res 27:649–656

[23] Aperador W, Bautista-Ruiz J, Chunga K (2015) Determination of the efficiency of cathodic protection applied to alternative concrete subjected to carbonation and chloride attack. Int J Electrochem 10:7073–7082

[24] Jeong J (2014) Cathodic prevention and cathodic protection of concrete slab with zinc sacrificial anode. Appl Mech Mater 597:341–344

[25] Carmona J, Garces P, Climent MA (2015) Efficiency of a conductive cement-based anodic system for the application of cathodic protection, cathodic prevention and electrochemical chloride extraction to control corrosion in reinforced concrete structures. Corros Sci 96:102–111

[26] Wen S, Chung DDL (2001) Effect of admixtures on the dielectric constant of cement paste. Cem Concr Res 31:673–677

[27] Wang Y, Chung DDL (2017) Effect of the fringing electric field on the apparent electric permittivity of cement-based materials. Compos B 126:192–201

[28] Sachdev VK, Sharma SK, Bhattacharya S, Patel K, Mehra NC, Gupta V, Tandon RP (2015) Electromagnetic shielding

performance of graphite in cement matrix for applied application. Adv Mater Lett 6:965–972
[29] Makul N (2013) Dielectric permittivity of various cement-based materials during the first 24 hours hydration. Open J Inorg Non Met Mater 3:53–57
[30] Simon D, Grabinsky MW (2012) Electromagnetic wave-based measurement techniques to study the role of Portland cement hydration in cemented paste backfill materials. Int J Min Reclam Environ 26:3–28
[31] Tsonos C, Stavrakas I, Anastasiadis C, Kyriazopoulos A, Kanapitsas A, Triantis D (2009) Probing the microstructure of cement mortars through dielectric parameters' variation. J Phys Chem Solids 70:576–583
[32] Abe Y, Asano M, Kita R, Shinyashiki N, Yagihara S (2008) Dielectric study on molecular dynamics in cement hydration. Trans Mater Res Soc Jpn 33:447–450
[33] Wang M, Chung DDL (2018) Understanding the increase of the electric permittivity of cement caused by latex addition. Compos B 134:177–185
[34] Knapen E, Van Gemert D (2011) Microstructural analysis of paste and interfacial transition zone in cement mortars modified with water-soluble polymers. Key Eng Mater 466(Polymers in Concrete):21–28
[35] Pichniarczyk P, Malata G (2017) Microcalorimetric analysis of methylcellulose influence on the hydration process of tricalcium aluminate, alite and their mixture. J Therm Anal Calorim 128(2):771–778
[36] Pichniarczyk P (2015) Influence of methylcellulose on the hydration of cement. Cem Wapno Beton 20(3):186–192
[37] Knapen E, Van Gemert D (2015) Polymer film formation in cement mortars modified with water-soluble polymers. Cem Concr Compos 58:23–28
[38] Pichniarczyk P (2013) The influence of methylcellulose on hydration of tricalcium aluminate. Cem Wapno Beton 18(2):65–73
[39] Knapen E, Van Gemert D (2009) Cement hydration and microstructure formation in the presence of water-soluble polymers. Cem Concr Res 39(1):6–13
[40] Ginzburg VV, Sammler RL, Huang W, Larson RG (2016) Anisotropic self-assembly and gelation in aqueous methylcellulose-theory and modeling. J Polym Sci B 54(16):1624–1636
[41] Coarna M, Georgescu M, Puri A, Diaconu D (2004) ESCA, MIP and mechanical characterization of some Portland cement-methyl-cellulose composites. Key Eng Mater 264–268(Pt. 3, Euro Ceramics VIII):2153–2156
[42] Lott JR, McAllister JW, Arvidson SA, Bates FS, Lodge TP (2013) Fibrillar structure of methylcellulose hydrogels. Biomacromol 14(8):2484–2488
[43] Silva DA, Monteiro PJM (2006) The influence of polymers on the hydration of portland cement phases analyzed by soft X-ray transmission microscopy. Cem Concr Res 36(8):1501–1507
[44] Shi X, Wang R, Wang P (2013) Dispersion and absorption of SBR latex in the system of mono-dispersed cement particles in water. Adv Mater Res (Durnten-Zurich, Switzerland) 687:347–353
[45] Wang M, Wang R, Yao H, Farhan S, Zheng S, Wang Z, Du C, Jiang H (2016) Research on the mechanism of polymer latex modified cement. Constr Build Mater 111:710–718
[46] Rottstegge J, Arnold M, Herschke L, Glasser G, Wilhelm M, Spiess HW, Hergeth WD (2005) Solid state NMR and LVSEM studies on the hardening of latex modified tile mortar systems. Cem Concr Res 35(12):2233–2243
[47] Yang Z, Shi X, Creighton AT, Peterson MM (2009) Effect of styrene-butadiene rubber latex on the chloride permeability and microstructure of Portland cement mortar. Constr Build Mater 23(6):2283–2290
[48] Vitorino FDC, Toledo Filho RD, Dweck J (2018) Hydration at early ages of styrene-butadiene copolymers cementitious systems. J Therm Anal Calorim 131(2):1041–1054
[49] Baueregger S, Perello M, Plank J (2015) Influence of carboxylated styrene-butadiene latex copolymer on Portland cement hydration. Cem Concr Compos 63:42–50
[50] Baueregger S, Perello M, Plank J (2015) Impact of carboxylated styrene-butadiene copolymer on the hydration kinetics of OPC and OPC/CAC/AH: the effect of Ca^{2+} sequestration from pore solution. Cem Concr Res 73:184–189
[51] Fu X, Chung DDL (1996) Effect of methylcellulose admixture on the mechanical properties of cement. Cem Concr Res 26(4):535–538
[52] Xu Y, Chung DDL (2000) Cement-based materials improved by surface-treated admixtures. ACI Mater J 97(3):333–342
[53] Fu F, Chung DDL (1996) Effect of polymer admixtures to cement on the bond strength and electrical contact resistivity between steel fiber and cement. Cem Concr Res 26(2):189–194
[54] Fu X, Chung DDL (1998) Improving the bond strength of concrete to reinforcement by adding methylcellulose to concrete. ACI Mater J 95(5):601–608
[55] Chen P, Fu X, Chung DDL (1997) Microstructural and mechanical effects of latex, methylcellulose and silica fume on carbon fiber reinforced cement. ACI Mater J 94(2):147–155
[56] Wang B, Zhang Y (2014) Synthesis and properties of carbon nanofibers filled cement-based composites combined with new surfactant methylcellulose. Mater Express 4(2):177–182

[57] Fu X, Chung DDL (1997) Effects of silica fume, latex, methylcellulose, and carbon fibers on the thermal conductivity and specific heat of cement paste. Cem Concr Res 27(12):1799–1804

[58] Benali Y, Ghomari F (2017) Latex influence on the mechanical behavior and durability of cementitious materials. J Adhes Sci Technol 31:219–241

[59] Zhong S, Chen Z (2002) Properties of latex blends and its modified cement mortars. Cem Concr Res 32:1515–1524

[60] Fu X, Chung DDL (1996) Degree of dispersion of latex particles in cement paste, as assessed by electrical resistivity measurement. Cem Concr Res 26(7):985–991

[61] Fu X, Chung DDL (1996) Vibration damping admixtures for cement. Cem Concr Res 26:69–75

[62] Fu X, Chung DDL (1998) Effects of water-cement ratio, curing age, silica fume, polymer admixtures, steel surface treatments, and corrosion on bond between concrete and steel reinforcing bars. ACI Mater J 95:725–734

[63] Issa CA, Assaad JJ (2017) Stability and bond properties of polymer-modified self-consolidating concrete for repair applications (Dordrecht, Netherlands). Mater Struct 50:1–16

[64] Keddam M, Takenouti H, Novoa XR, Andrade C, Alonso C (1997) Impedance measurements on cement paste. Cem Concr Res 27(8):1191–1201

[65] Andrade C, Blanco VM, Collazo A, Keddam M, Novoa XR, Takenouti H (1999) Cement paste hardening process studied by impedance spectroscopy. Electrochim Acta 44(24): 4313–4318

[66] Chung DDL (2010) Functional materials. World Scientific Publishing, Singapore

[67] http://msdssearch.dow.com/PublishedLiteratureDOWCOM/dh_08e5/0901b803808e5f58.pdf?filepath=dowwolff/pdfs/noreg/198-02289.pdf&fromPage=GetDoc. Accessed 22 Feb 2017

[68] https://www.vega.com/home_ss/-/media/PDF-files/List_of_dielectric_constants_EN.ashx. Accessed 22 Feb 2017

[69] http://scientificpolymer.com/density-of-polymers-by-density/. Accessed 6 May 2017

[70] Riddle B, Baker-Jarvis J, Krupka J (2003) Complex permittivity measurements of common plastics over variable temperatures. IEEE Trans Microw Theory Tech 51:727–733

[71] Kampouris DK, Ji X, Randviir EP, Banks CE (2015) A new approach for the improved interpretation of capacitance measurements for materials utilised in energy storage. RSC Adv 5(17):12782–12791

[72] Macdonald JR (1990) Impedance spectroscopy: old problems and new developments. Electrochim Acta 35(10):1483–1492

[73] Kisza A, Kazmierczak J, Meisner B (2004) The influence of the experimental setup upon the modelling of the impedance spectra in molten salts. Pol J Chem 78(9):1235–1244

[74] Dinulovic M, Rasuo B (2009) Dielectric properties modeling of composite materials. FME Trans 37:117–122